We are IntechOpen,
the world's leading publisher of
Open Access books
Built by scientists, for scientists

6,900
Open access books available

186,000
International authors and editors

200M
Downloads

Our authors are among the

154
Countries delivered to

TOP 1%
most cited scientists

12.2%
Contributors from top 500 universities

Interested in publishing with us?
Contact book.department@intechopen.com

Numbers displayed above are based on latest data collected.
For more information visit www.intechopen.com

Structural Characterisation of Kraft Pulp Fibres and Their Nanofibrillated Materials for Biodegradable Composite Applications

Gary Chinga-Carrasco[1], Arttu Miettinen[2], Cris L. Luengo Hendriks[3],
E. Kristofer Gamstedt[4] and Markku Kataja[2]

[1]*Paper and Fibre Research Institute (PFI),*
[2]*Department of Physics, University of Jyväskylä,*
[3]*Centre for Image Analysis, Swedish University of Agricultural Sciences,*
[4]*The Ångström Laboratory, Uppsala University,*
[1]*Norway*
[2]*Finland*
[3,4]*Sweden*

1. Introduction

The utilization of wood pulp fibres in composite materials has gained major interest during the last years. One of the major motivations has been the potential of wood pulp fibres and their nanofibrillated derivatives for increasing the mechanical properties of some materials. However, in order to exploit the full potential of wood pulp fibres and cellulose nanofibrils as reinforcement in hydrophilic and hydrophobic matrices, several characteristics of fibres and their interactions with a given matrix need to be understood.

With the increasing capabilities of novel microscopy techniques and computerized image analysis, structural analysis is moving forward from visual and subjective evaluations to automatic quantification. In addition, several microscopy techniques for obtaining 2D and 3D images of a given composite material, including field-emission scanning electron microscopy (FESEM) and X-ray micro-computed tomography (X-μCT), have evolved considerably during the last years. X-μCT is a non-destructive method for obtaining the three-dimensional structure of a physical material sample. It is well suited for structural analysis of complex heterogeneous materials such as paper, biological materials and fibrous composites (Samuelsen *et al.*, 2001; Holmstad *et al.*, 2005; Axelsson, 2008). In addition, FESEM is a powerful technique for assessment of a variety of materials. One of the major advantages of FESEM is its versatility and high-resolution power (Chinga-Carrasco *et al.*, 2011). Structures down to 1-2 nm can thus be visualized and quantified.

In this work we will focus on practical and complementary imaging and image analysis techniques. We will also give a brief introduction to SEM, X-μCT and to 3D image analysis methods, emphasizing topics that are relevant for characterisation of composite materials. Selected case studies of wood pulp fibre-reinforced composite materials and their corresponding microstructure-property relationships will be discussed.

2. Wood pulp fibres and microfibrillated cellulose

Wood pulp fibres (Fig. 1) are regaining interest within several industry sectors. Wood pulp fibres are a natural resource, renewable and biodegradable. This is a major advantage in a world moving towards environmental-friendly products, where major efforts are being made to develop sustainable materials. Considering sustainability and recyclability as major requirements, wood pulp fibres are ideal components for novel composite materials.
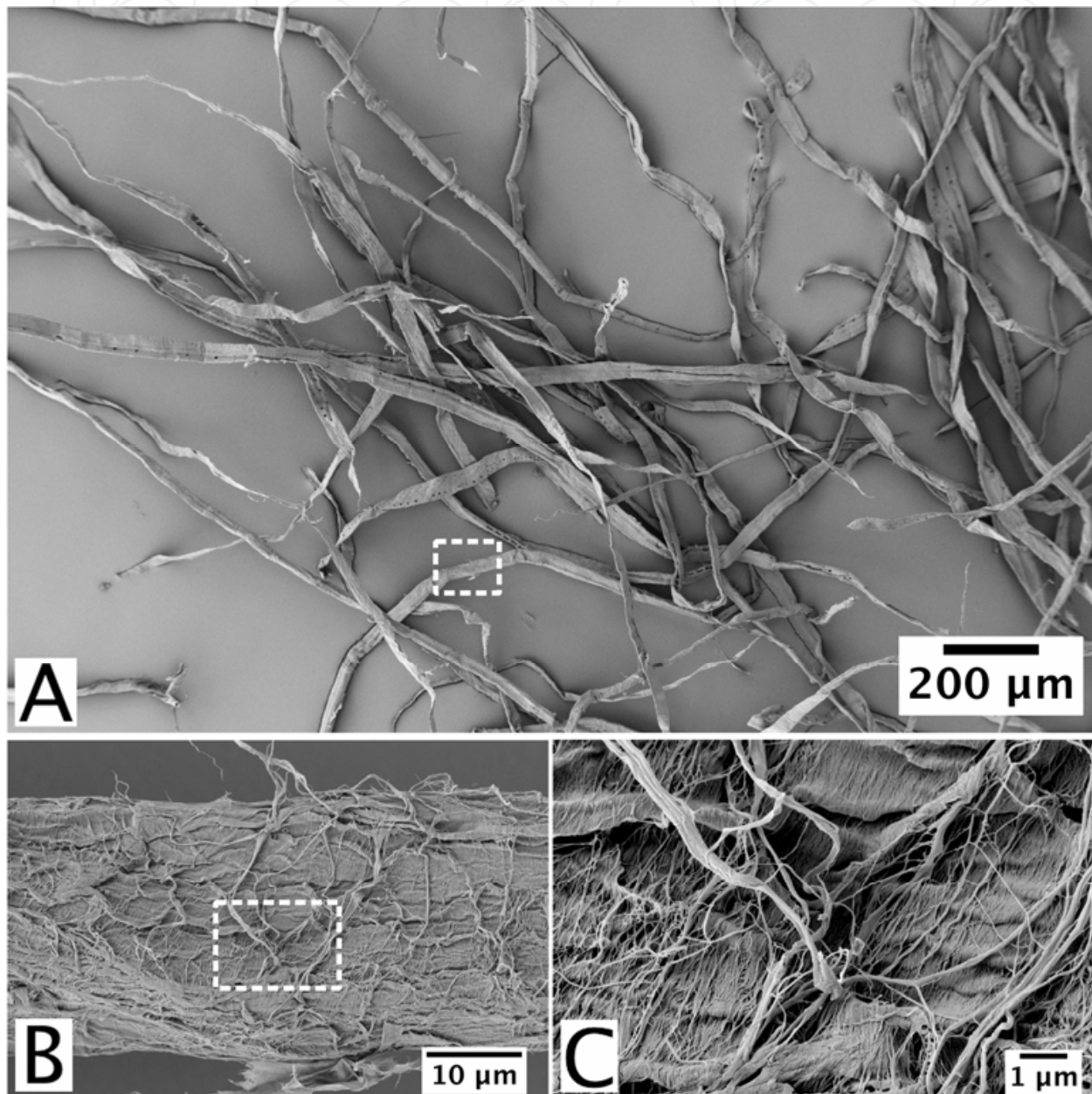

Fig. 1. FESEM of the structure of kraft pulp fibres. (A) Kraft fibres exemplifying their high aspect ratio. (B) A surface structure of a single fibre. (C) The microfibrils composing the surface structure. The dashed rectangles in (A) and (B) correspond to the images in (B) and (C), respectively.

Structural Characterisation of Kraft Pulp Fibres and Their
Nanofibrillated Materials for Biodegradable Composite Applications

245

Wood pulp fibres have a relatively high aspect ratio. Typical lengths are between 1 and 3 mm (Fig. 1A). Typical widths are between roughly 10 and 50 μm (Fig. 1B). The wall structure of cellulose fibres is mainly composed of microfibrils, with reported values of diameter in the nanometer-scale (Fig. 1C). The microfibrils are arranged differently in the various layers of a fibre wall structure (see *e.g.* Meier, 1962; Heyn, 1969). The wall of cellulose fibres is roughly composed of a primary wall and 3 secondary wall layers, *i.e.* S1, S2 and S3.

Cellulose fibres can also be disintegrated into their structural nano-components. This approach was introduced in the beginning of the eighties for commercial purposes (Turbak *et al.*, 1983; Herrick *et al.*, 1983). The novel material was denominated microfibrillated cellulose (MFC). The material has also been given a series of different denominations, including nanofibrillated cellulose, nanofibrils, nanofibres and nanocellulose (Abe *et al.*, 2007; Ahola *et al.*, 2008; Mörseburg & Chinga-Carrasco, 2009; Klemm *et al.*, 2010). MFC can be considered a nano-material, provided that the material is composed of a major fraction of individualized nanofibrils (Fig. 2). In this study, nanofibrils are considered the material produced through a homogenization process, having at least one dimension less than 100 nm.
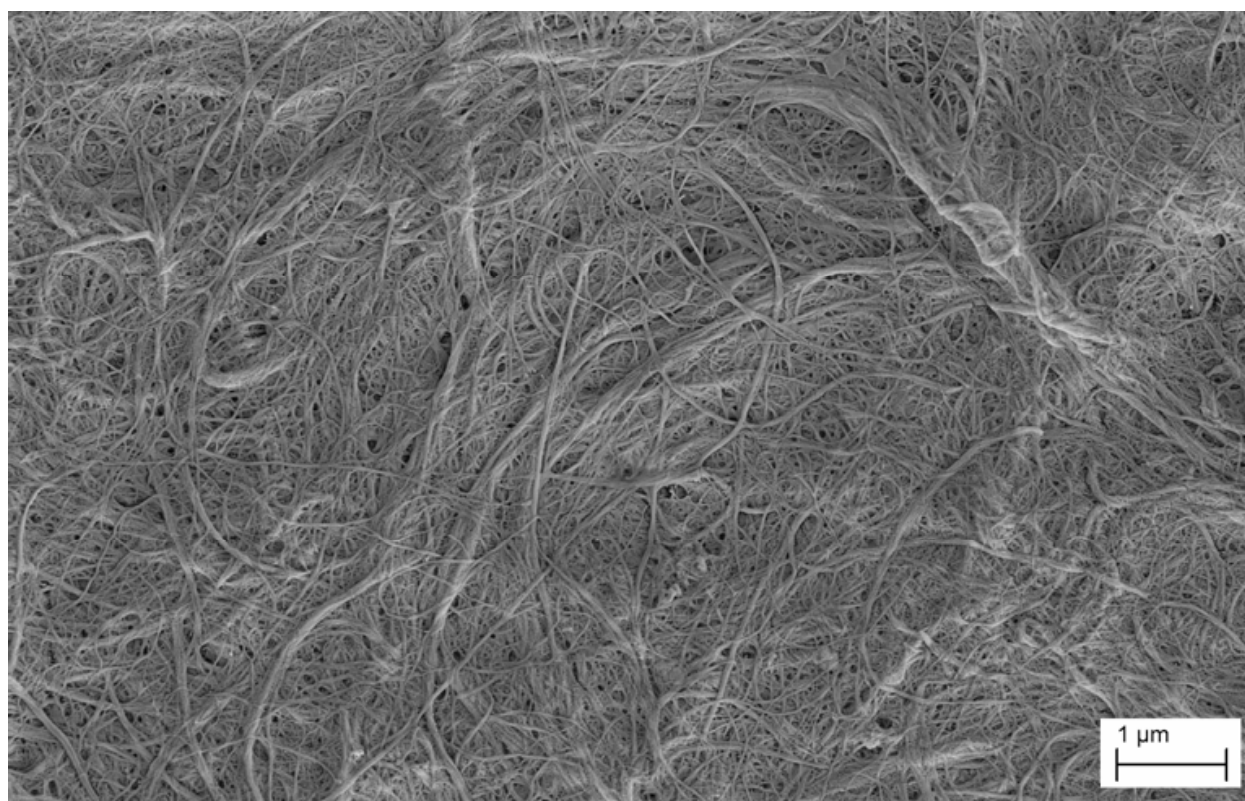

Fig. 2. FESEM image of microfibrillated cellulose, produced from kraft pulp fibres . The material is composed mainly of cellulose nanofibrils.

A series of new approaches have been developed for production of MFC (Saito *et al.*, 2006; Päkkö *et al.*, 2007; Wågberg *et al.*, 2008). The procedure for producing MFC may include mechanical, enzymatic and chemical pre-treatments. Each pre-treatment seems to produce a material with different morphology and different diameter size distribution. Depending on the applied amount of energy, homogenization without pre-treatment may produce a

material containing nanofibrils, fibre fragments and poorly fibrillated fibres. On the other side, chemi-mechanical pre-treatments yield a narrow nanofibril diameter size distribution. This has been considered a confirmation of the positive effect that chemi-mechanical pre-treatments have on facilitating the fibrillation of cellulose fibres (see Syverud *et al.*, 2010).

3. Production of fibre-reinforced composites and cellulose nanofibrils

In this chapter, kraft pulp fibres (Fig. 1) will be applied as reinforcement in a fibre-polylactic acid (PLA) composite material and as a source for production of cellulose nanofibrils (Fig. 2).
A homogenization process was applied for producing cellulose nanofibrils (Fig. 2). The kraft pulp fibres were beaten prior to the homogenization. The homogenization was performed with a Rannie 15 type 12.56X homogenizer operated at 1000 bar pressure. The pulp consistency during homogenizing was 1%. The fibrillated material was collected after 3 passes through the homogenizer.
The following procedure was applied for production of fibre-PLA composites. The kraft pulp fibres were pelletized before manufacturing the composites. The applied equipment was a Kahl flat die pelletising press (Kahl 14-175, Reinbek, Germany). For details on the procedure see Nygård *et al.* (2008). Composites of PLA reinforced with 10%, 30% and 40% kraft fibre loadings were produced. The kraft pulp fibres and PLA were blended in a compounding unit (double screw) equipped with an injection moulding unit. Dogbone samples were made by injection moulding.

4. Structural characterisation

Proper structural characterization of cellulose fibres, nanofibrils and their corresponding composite materials requires an adequate utilization of specialized equipment for detailed assessments. In this respect it is most important to be aware of the advantages and limitations of modern microscopy techniques, and apply their complementary capabilities. In this work we emphasize the complementary capabilities of X-μCT for 3D characterization and SEM for complementary assessments at the micro and nano-scales. While X-μCT requires none or minor sample preparation, electron microscopy techniques may require adequate preparation for exposing a given structure. In the following sections, some of the techniques applied for fibre structural characterization will be described.

4.1 Scanning electron microscopy (SEM)
SEM has several modes of operation, from conventional secondary electron imaging (SEI) mode for studying fibre surfaces to specialized field-emission SEM (FESEM) for assessment of nano-structures. Image acquisition from fibre surfaces requires none or minor preparation. The fibre samples may be covered with a conductive metallic layer. Uncoated fibre samples may also be visualized with environmental or low-vacuum SEM. Well-prepared fibre samples reveal structures in the nanometre scale, such as the microfibrils observed in fibre wall structures (Fig. 1C).

4.1.1 Preparation for electron microscopy
One of the principal objectives with preparation techniques is to preserve a given structure in a particular state. Preparation is especially necessary for several electron microscopy techniques.

Structural Characterisation of Kraft Pulp Fibres and Their
Nanofibrillated Materials for Biodegradable Composite Applications

247

In the case of wood pulp fibres, dedicated preparation techniques have been developed. This includes *e.g.* freeze-drying, cryofixation and critical point drying (de Silveira *et al.*, 1995; Duchesne and Daniel, 2000). Freeze-drying is relatively simple to perform and has been applied in this study as a step in the preparation of the kraft pulp fibres.

Freeze-drying has facilitated the preparation of single fibres and bundles of fibres for surface structural analysis in SEI mode (Fig. 1; Chinga-Carrasco *et al.*, 2010). In addition, SEM in backscatter electron imaging (BEI) mode has been applied for cross-sectional analysis (Reme *et al.*, 2002; Chinga-Carrasco *et al.*, 2009). The SEM-BEI mode yields contrast based on the local average atomic number of a given structure. SEM-BEI mode requires distortion-free and smooth surfaces of the studied samples. A well-established method consists on i) embedding in epoxy resin, ii) grinding using abrasive papers and iii) polishing with a cloth using a fine diamond paste (Reme *et al.*, 2002). If modern equipment is available, blocks can be prepared quickly and effectively. This is a major advantage, as the cross-sectional structural characteristics of large fibre populations can be quantified (Fig. 3). The quantification of fibre cross-sectional characteristics is of importance in several applications such as; i) verification of fibre development due to different pulping processes, ii) evaluation of pre-treatments (*e.g.* enzymatically, chemically) on the fibre morphology, for homogenization purposes and iii) assessment of the relationship of fibre morphology and composite characteristics.
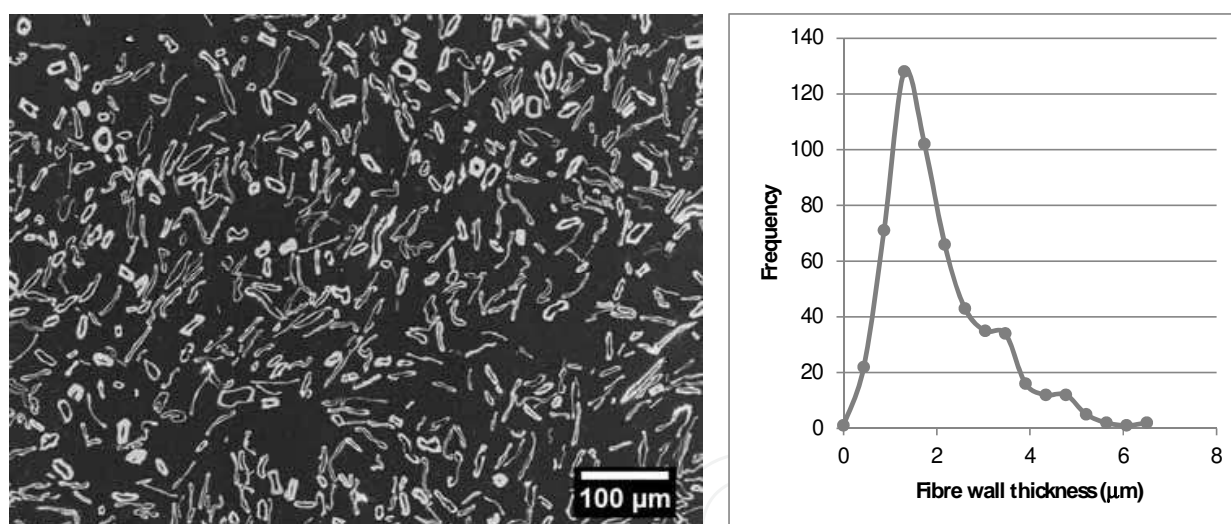

Fig. 3. SEM analysis of fibre cross-sections. (Left) Cross-sectional image acquired in backscattered electron imaging mode. (Right) The fibre wall thickness distribution of the kraft fibres applied in this study. See also Chinga-Carrasco *et al.* (2009).

4.2 X-ray micro-computed tomography (X-μCT)

Tomographic imaging facilities, based on synchrotron radiation and capable of resolution in the micrometre range, have been in use for more than a decade. During the past few years, the techniques have developed rapidly towards higher resolution. Furthermore, table-top tomographic scanners based on x-ray tube have become available. Depending on the techniques used, the resolution of the 3D tomographic images can vary from millimetres down to a few tens of nanometres (Fig. 4). In structural analysis of *e.g.* composite materials, resolution of the order of a micrometre is typically used. Such

resolution is generally available also with current commercial tomographic table-top scanners.
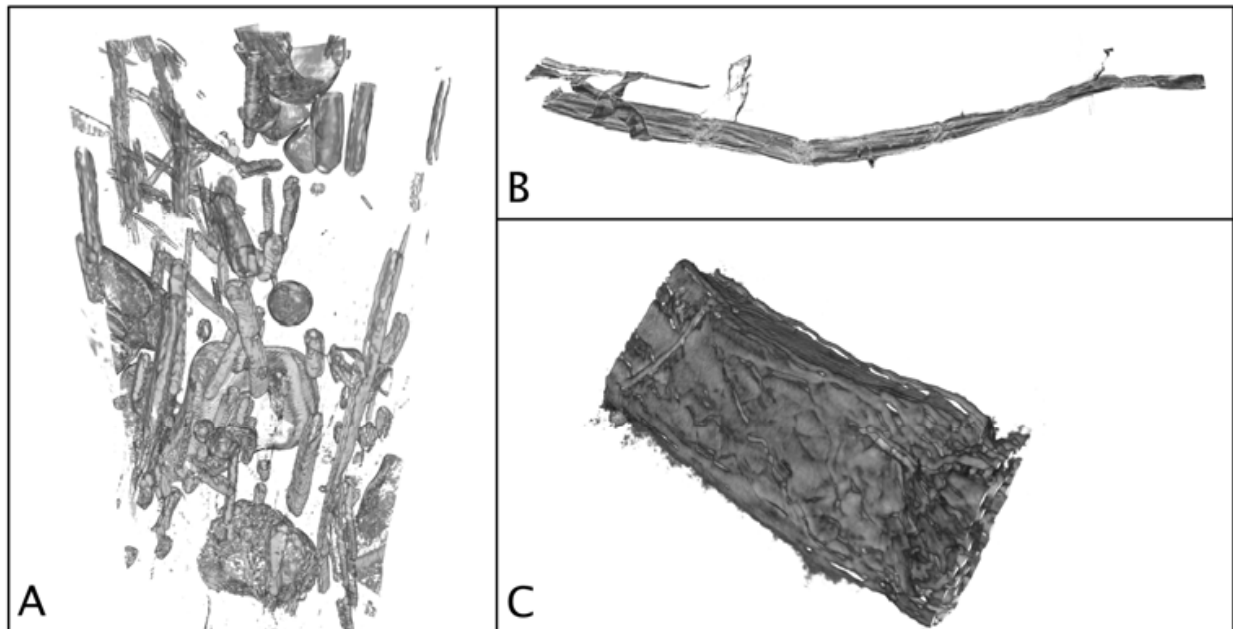

Fig. 4. X-µCT images acquired at different scales. (A) Wood fibre composite material, only fibres and some air bubbles are visible. The height of the sample is about 420 µm. Note that long fibres (Fig. 1A) are cut by the edges of the image. (B) Single wood fibre whose length is about one millimetre. (C) About 150 µm long part of a single wood fibre showing fibrils on the surface of the fibre. The images were acquired at ESRF ID19 synchrotron beamline (A), using XRadia microCT device (B) and using XRadia nanoCT device (C).

The basic components of a typical X-µCT apparatus are the x-ray source, object stage, scintillator plate and CCD camera. Some devices include additional optical systems for x-rays or for visible light. The entire device also contains a computer system for data acquisition and for reconstruction. Tomographic imaging is done by firstly acquiring a series of x-ray images of the object from several directions. Typically, of the order of 1000 individual x-ray images are taken while the object is rotated in small angular steps for 180 degrees around a vertical axis. These two-dimensional projection images are then processed computationally to reconstruct a three-dimensional digital image of the structure. Two different modalities of x-ray tomography are generally used, *i.e.* absorption mode and phase contrast mode. Within the absorption mode tomography, the numerical value associated with each 'voxel' in the reconstructed 3D image represents the local value of x-ray absorption coefficient of the material. For non-crystalline (non-diffractive) materials the absorption coefficient correlates with the density of the material. Consequently, an absorption mode tomographic image of such a material may be interpreted as an approximation of the density distribution within the sample. Interpretation of a phase contrast tomographic image is more complicated. In general, such an image emphasizes regions of high density gradient, *e.g.* intrinsic surfaces between various components in a composite material. In the following we will concentrate on absorption mode X-µCT.

An important advantage of the X-µCT method is that no particular sample preparation is needed. Consequently, material samples can be imaged under various conditions with respect to *e.g.* humidity, state of deformation, *etc.* The same physical sample may also be scanned several times in different conditions and studied with other, complementary methods. In addition to giving a graphical visual view on the structural characteristics of heterogeneous materials, the tomographic images can be utilized to obtain detailed quantitative information. Various segmentation and 3D image analysis methods have been developed for *e.g.* separating various components of the heterogeneous material and analysing them individually for structural properties such as relative volume, spatial distribution, domain size and shape distributions, specific area, connectivity, orientation, *etc.* Combining X-µCT with numerical simulation enables more advanced analysis of also dynamic characteristics such as transport and elastic properties of materials. A noteworthy further advantage of the method is that various analyses of quite different nature can be made based on the same basic data, *i.e.* the 3D digital image of the actual material structure.

4.3 Image processing and analysis

Depending on the particular device for image acquisition, digital images may contain varying amounts of noise, which must be removed before using the images for further analysis. In the case of X-µCT, several algorithms for such filtering have been developed (Jähne, 2002). One of the simplest adaptive filters is the variance weighted mean filter (Gonzalez & Woods, 2002), based on the assumption that the local variance of grey value is higher near edges of internal structures or domains than in the bulk far away from the edges. Another common noise removal method is the bilateral filter which is based on replacing the value of each pixel with a weighted average of values of the surrounding pixels (Tomasi & Manduchi, 1998). The weight function is a Gaussian function that depends on the Euclidean distance and on the grey value distance from the centre pixel. In addition, the non-linear SUSAN (Smallest Univalue Segment Assimilating Nucleus) filter (Smith and Brady, 1997), which is similar to the bilateral filter, has proven to be suitable for noise-removal in X-µCT images of wood fibre composites (Axelsson, 2009).

Successful noise removal facilitates many straightforward analyses on digital images. For example, the fibre content in a composite material can be estimated simply by segmenting the image into fibre pixels and background pixels based on a suitable threshold value, and by calculating the ratio of the number of fibre pixels to the number of all pixels. In the case of X-µCT analysis, this requires that the values of the x-ray absorption coefficient (density) of the fibres and the matrix are sufficiently distinct such that a successful thresholding becomes possible.

As mentioned above, various characteristics of fibre-reinforced composites can be quantified, including fibre spatial distribution, fibre orientation and volume fraction. In addition, the fibre and nanofibril lengths are of major importance as these characteristics affect some critical mechanical properties of a given composite material. Methods for quantification of fibre and nanofibril lengths are described in the following sections.

4.3.1 Quantification of fibre length distribution

The fibre length distribution of a composite material is a basic quantity that is often needed for microstructural modelling or for optimization of processing parameters in the

manufacturing phase. Finding the fibre length distribution of a material from a three-dimensional image is a nontrivial problem. In this section we present a two-phase algorithm for such analysis.

Before proceeding further, let us consider the problem of measurement of fibre length from a finite volume such as an X-µCT image. The measurement will be affected by the edges of the volume, which cut long fibres into shorter segments (see Fig. 4A and Fig. 6). Additionally, the probability of a randomly positioned fibre being in the volume is related to the length of the fibre and to the size of the finite volume. Thus, the fibre length distribution measured from a finite volume and the true fibre length distribution in the sample material do not coincide. This effect can be corrected for by utilizing a linear measurement model of the fibre length distribution. This indicates the relation

$$m = \alpha n + \epsilon \, ,$$

where m is the fibre length distribution measured from the image, n is the actual fibre length distribution in the sample material, ϵ is a random error vector and α is a matrix that describes the measurement process. The correction is performed by solving the equation for n using, *e.g.* Tikhonov regularization. For details on the matrix α and the solution process, see Miettinen *et al.* (2011).

The method for measuring fibre length is based on a granulometry approach. The granulometry is a well-established tool to characterise texture by the size of its components (Matheron, 1975; Soille, 2003). The granulometry is, in essence, a multi-scale version of the mathematical morphology operations of opening or closing. It applies an opening (or closing) at many different scales, and summarises the result of each operation by summing the grey values of the output image. When applied to a properly prepared image, and with careful normalisation, it yields an estimate of the size distribution of the objects in an image (Luengo Hendriks, 2004). The size of an object can be defined by a suitably chosen opening (or closing) operation. Most commonly, isotropic openings are used. These use the object's width as its size. Another common possibility is the area opening, which uses the object's volume. We propose to use the path opening (Luengo Hendriks, 2010), which selects on the object's length. Applying granulometry with path openings on suitable images with fibres thus yields an estimate of the fibre length.

4.3.2 Quantification of fibril length

Proper homogenisation of kraft pulp fibres yields fibrillated materials, which are composed of a major fraction of cellulose nanofibrils (Fig. 2). The diameters of cellulose nanofibrils are in the nanometre scale (< 100 nm). The quantification of nanofibril diameters has been applied for evaluating the fibrillation of a given pulp and how this is affected by a given pre-treatment before homogenisation (see *e.g.* Chinga-Carrasco *et al.*, 2011). In addition to the nanofibril diameter as a structural characteristic, the quantification of the corresponding nanofibril length is most important. However, quantification of the nanofibril length is demanding. This is due to the morphology of the nanofibrils, which may have diameters and lengths in the nanometre and micrometre-scale, respectively. Visualization of nanofibrils requires high-resolution and large field of view. In order to fulfil these requirements a proposed approach is to acquire several adjacent high-resolution images

Structural Characterisation of Kraft Pulp Fibres and Their
Nanofibrillated Materials for Biodegradable Composite Applications

251

with a FESEM and stitch them digitally (Fig. 5A). The image exemplified in Fig. 5 is composed of various adjacent and stitched images. The images were then filtered with a Fast Fourier Transform (FFT) bandpass filter to preserve the structures corresponding to the fibrillated materials.

SEM images may be difficult to analyse automatically. The contrast in SEM-SEI images is obtained, not through differences in surface properties as in optical imaging, but through orientation of the surface and shadowing effects. This means that the brightness of a pixel is not related to material properties, but to local geometry in the sample. In the acquired images, pixels corresponding to the nanofibrils have slight differences with respect to the intensity of the background. Human vision is particularly adept at interpreting this type of image, but it is deceptively tricky to teach a program to do the same. This is the so-called "shape from shading" problem, well studied in the computer vision literature (Zhang, 1999). However, applying such computer vision techniques to SEM images yields unreliable results (Czepkowski, 1996).
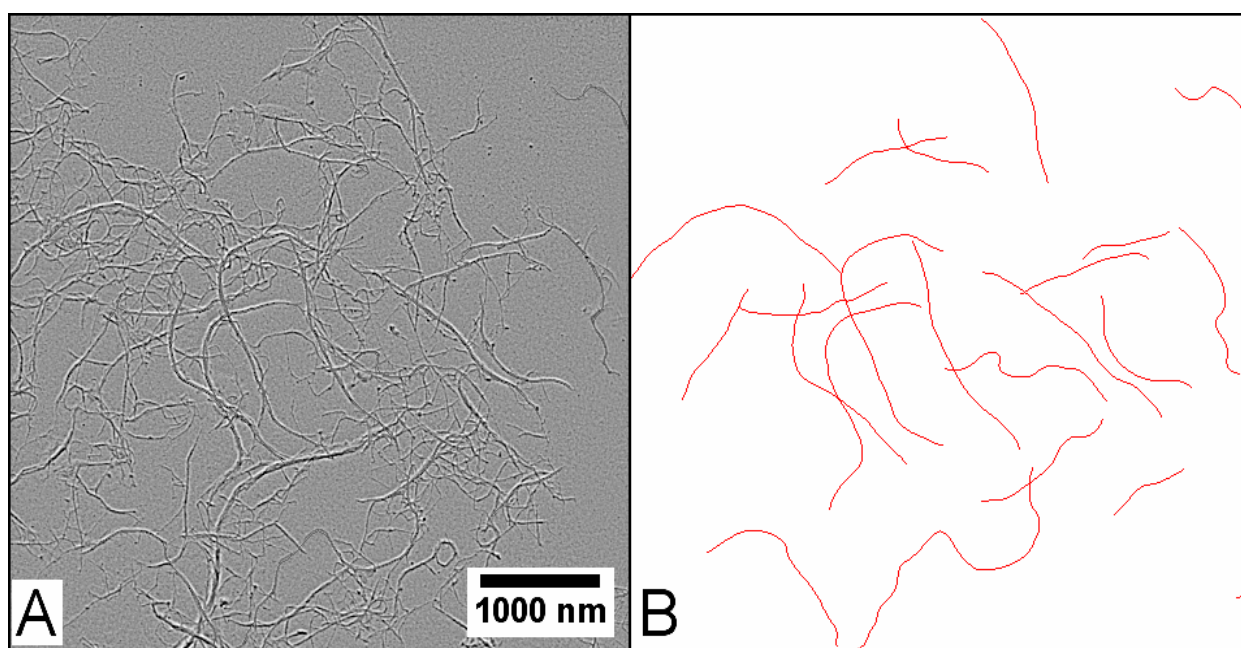

Fig. 5. Quantification of nanofibril lengths based on FESEM images. (A) Digital image acquired in SEI mode. The image has been enhanced for better visualization. (B) The corresponding processed image with paths drawn on some nanofibrils.

In this chapter we propose a semi-automated approach to measuring nanofibrils with high accuracy. Through a simple user interface, the analyst clicks on the two ends of a fibril. The software can then compute an optimal path between those two positions, and draw the path over the image. The analyst can then refine the path through additional clicks. This may be necessary only in specific situations, such as with strongly bent fibrils and fibrils that intersect at multiple locations. Once the fibril is found, an accurate length measurement can be calculated.

The following procedure was applied for detecting the nanofibrils exemplified in Fig. 5. First, we inverted the grey values in the image, such that the shadow regions were

represented by high grey values. Next, we determined the optimal path between two points. A path is a sequence of neighbouring pixels, such that the first and last pixels in the path are the points selected by the analyst. We defined the optimal path as the path over which the integrated grey value were minimal. That is, if a path deviated from the fibril and went across a shadow region, it would yield a larger grey value integral than a path that nicely followed the fibril. Optimal path finding is a well-studied problem, and can be solved with a famous algorithm due to Dijkstra. In the image analysis world, the grey-weighted distance transform (GWDT) is the best-known version of the Dijkstra algorithm (Verbeek and Verwer, 1990). We applied the GWDT to compute the grey-weighted distances to one of the two selected points, and then, starting at the other point, found the path of steepest descent, which always takes one back to the first point. This path necessarily corresponds to the optimal path according to our criterion. When corrections were necessary, the analyst added control points. In this case, we found the optimal path between subsequent points, and appended these paths to obtain a trace of the whole fibril. This path was thus composed of a dense set of points, one pixel apart, and represented by the coordinates of these points (Fig. 5).

Measuring the length of the path can be accomplished by first smoothing the path. The sequence of x and y coordinates was filtered using a Gaussian low-pass filter with an appropriate sigma (σ) value. We found that $\sigma = 3$ yielded good results and this value was applied for smoothing the path. Next, the Euclidean distance between subsequent points was calculated and summed. Summing the Euclidean distance in this way overestimates the length if the path has not been smoothed (Vossepoel and Smeulders, 1982). Finally, the length in pixels can be converted to a physical length by multiplying with the pixel size.

In this section we have described a method that may be used for quantification of nanofibril length, although the approach is demanding. The approach will be improved, considering (i) adequate procedures for sample preparation of well-dispersed nanofibrils, (ii) alternative methods for image acquisition, *e.g.* transmission electron microscopy and (iii) alternative and improved methods for nanofibril tracking and quantification.

5. The effect of fibres and nanofibrils on the mechanical properties of composite materials

All of the above examples of fibre and fibril length are of great importance for the mechanical properties of the composites or networks composed of fibres or fibrils. Structural composites for load-carrying applications are based on long fibres acting as reinforcement, whereas high-volume composites with particle 'reinforcement' are preferred to reduce costs by using cheaper filler or to improve processability. For new cellulose-based materials with improved mechanical properties, it is therefore of interest to control the length of the reinforcement. Microscopic techniques to quantify fibre length distribution are therefore of practical interest.

Essentially it is the aspect ratio of a cylindrical fibre, *i.e.* its length to diameter ratio, which controls the average load in the fibre. This is perhaps best illustrated by an oriented fibre embedded in a softer matrix, which is subjected to a far-field stress in the direction of the fibre. Since load is transferred from the matrix to the fibre at the interface by shear stresses, there will be ineffective lengths at the fibre ends, where build-up in fibre tensile stress takes

place. In parallel, processing methods should be developed to manufacture larger quantities at lower cost, while maintaining proper control of the microstructure to assure improved mechanical properties. This balance between processability and performance is an omnipresent challenge in development of materials of this kind. Hence, compromises between processability and performance have to be considered. A particular feature of wood pulp fibres is that they are easily dispersed in water and that they form strong bonds to each other upon drying, which is not the case for other typical composite fibres, such as glass or carbon fibres. This behaviour could potentially be utilized as a processing advantage, using wet forming techniques and water suspensions in mixing the composite constituents. Experience in the paper making community could be used to manufacture novel composites, in combination with processing techniques presently used to manufacture polymer matrix composites.

Wood-plastic composites (WPCs), based primarily on extruded wood flour filled polyolefins, have a large market as building components in North America. The aspect ratio of the wood reinforcement is typically low (below 5). The resulting mechanical properties are therefore limited, since the wood particles may act as stress raisers rather than load-carrying fibres. The aspect ratio is a critical microstructural parameter that controls stiffness and strength, which should be increased for WPCs (Fowler *et al.*, 2006). The pivotal role of fibre length is perhaps best illustrated by the concept of ineffective length introduced by Cox (1953). For an embedded fibre oriented along the direction of load, there are short distances close to the two fibre ends that do not carry full load, since stress is transferred by interfacial shear from the fibre ends. The effect of fibre length or aspect ratio on mechanical properties is large for small values, but then reaches an asymptotic value. Above a certain value of the aspect ratio, say ~ 20, further increase might not be worth the slight improvement in stiffness and strength (Nordin, 2004). The desired increase in fibre length, compared to WPCs, has prompted use of wood pulp fibre reinforcement, where the wood tracheids could have an aspect ratio of 60 or more (McHenry & Stachurski, 2003). Although the pulp fibres have sufficiently high aspect ratios, conventional melt processing of wood-fibre reinforced polymers usually degrades the fibre length to the extent that it adversely affects the mechanical properties (Almedar *et al.*, 2008). This motivates the development of the above-mentioned techniques to quantify fibre length for wood-fibre composites. Fibre length is known to affect several important engineering properties of composites. Several models, with experimental support, have been developed to link the fibre length to some key engineering properties:

- Stiffness, according to shear-lag model of Cox (1953)
- Tensile strength, according to the model Fukuda & Chou (1981), although fibre dispersion may overshadow the fibre-length effects since wood fibres tend to aggregate on drying
- Fracture toughness, according to the model of Piggott (1970)
- Dimensional stability on moisture uptake, according to the model by Almgren *et al.* (2010), where increased stiffness is shown to constrain swelling

All of these engineering properties are considered in materials selection and design, depending on the application at hand. It is not only the fibre length and its distribution that affects these properties. Obviously, the fibre orientation distribution and fibre content are of great importance (Fig. 6). These parameters are however relatively easier to characterize by

image analysis. Efforts to develop methods for fibre length characterization are therefore most important.
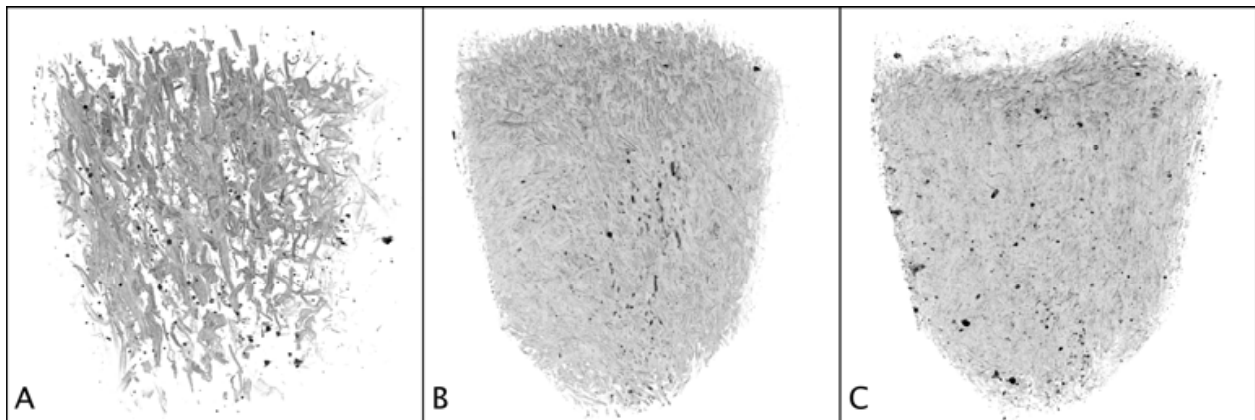

Fig. 6. X-µCT images of kraft fibre-PLA composites, consisting of 10 weight-% (A), 30 weight-% (B) and 40 weight-% of fibre (C). The images were acquired with XRadia microCT device.

In this chapter we have described a method based on granulometry for quantification of fibre length in X-µCT 3D images (see section 4.3.1). The method appears robust and yields reasonable results. The quantification of fibre length in the samples presented in Fig. 6 yields values of length below 200 µm. The fibre length distributions are relatively broad, ranging from small (<10 µm) to relatively long fibre fragments (100-200 µm). It is worth to mention that the kraft fibres had an average fibre length of 1690 µm before composite manufacturing (measured with a FiberMaster device). This clearly indicates that the process applied for manufacturing the composite material has shortened the fibre length, which reduces the corresponding mechanical strength (for details see Miettinen *et al.*, 2011).

As discussed above, the geometrical variability of natural wood fibres imposes challenges on the development of robust methods for quantification of fibre length in composite materials. Such quantification is demanding and requires tailor-made algorithms for a given application. There is thus scope for scientific research work in this domain, especially within non-destructive quantification of fibre morphology in composite materials.

An additional example of the application of X-µCT in the study of the properties of wood fibre reinforced composite materials is shown in Fig. 7. In this particular case, the entire test specimens (dogbones) of the material were first imaged using X-µCT to find the distribution of possible defects and irregularities. Mechanical tests were then performed to determine the stress-strain curve and tensile strength. After tensile testing, the fractured regions were imaged again using both X-µCT (Fig. 7) and SEM (Fig. 8). Comparison of the X-µCT images taken before and after the tensile test allowed identifying the critical structural features leading to fracture (Fig. 7). It appears that relatively large fibre agglomerates seem to have initiated the failure and crack propagation. The agglomerates, which are poorly dispersed fibres in the PLA matrix, were confirmed by SEM images (Fig. 8). Fractography based on SEM is a relatively

common technique for failure analysis (see *e.g.* McCoy, 1994; Hein, 2001). The fracture area clearly showed the occurrence of local areas with higher concentration of fibres (Fig. 8C), compared to neighbouring regions (Fig. 8B). The case-study presented in this section exemplifies the complementary capabilities of two modern techniques for structural analyses, *i.e.* X-μCT and (FE)SEM.
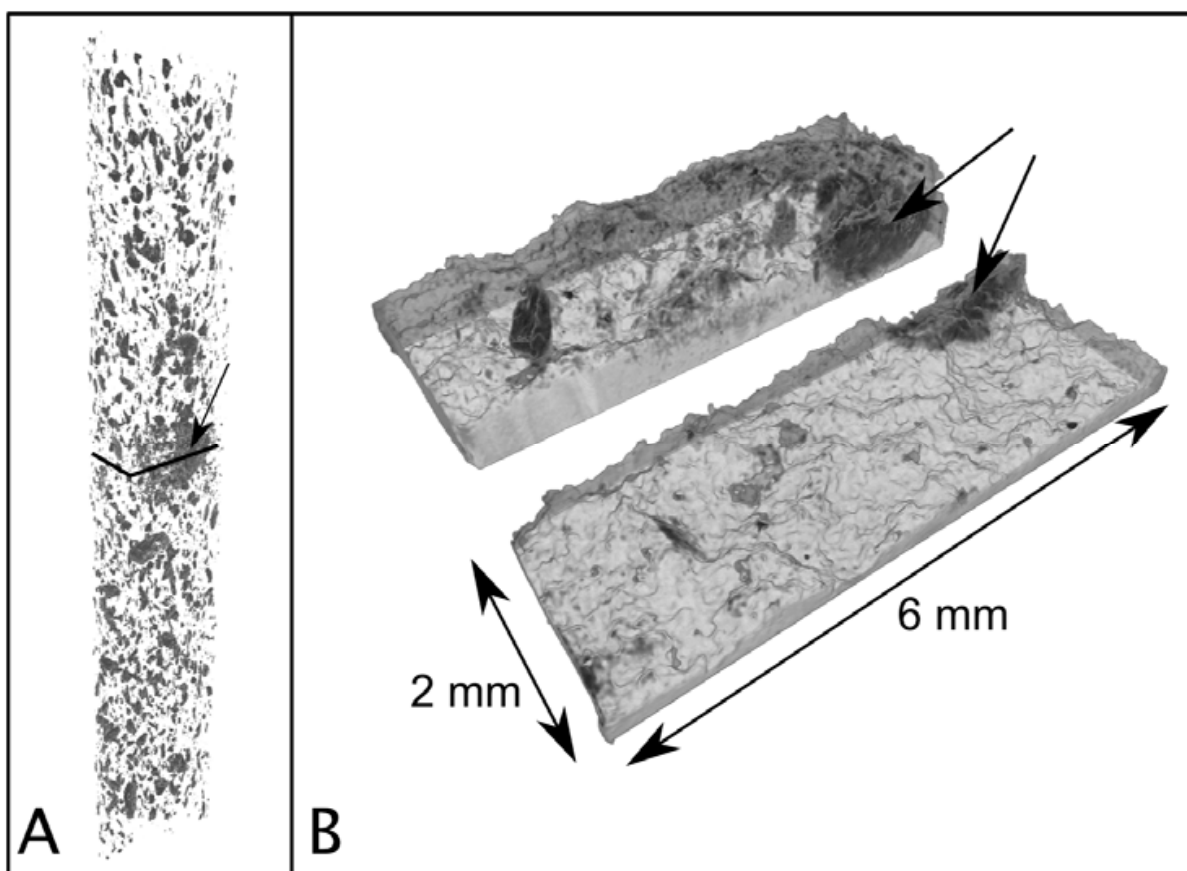

Fig. 7. X-μCT images of a kraft fibre-PLA composite sample (dogbone) of approximate dimensions 60 mm × 6 mm × 2 mm. The images have been acquired with a SkyScan 1172 tabletop tomography device. (A) Fibre bundles inside the intact specimen. (B) Fracture surfaces after tensile testing. The arrows in (A) and (B) indicate the critical defect (dark area) that caused the failure of the structure. The black line in A) indicate the approximate position of the fracture.

These structure-property relations essentially apply also to the corresponding nanofibrils, made from kraft pulp fibres. The main difference is the dimension and the specific surface area. The aspect ratio depends on the fibrillation procedure, although it is possible to produce sufficiently long nanofibrils that they can be considered continuous, *i.e.* of indefinite length from a load-carrying perspective (Henriksson *et al.*, 2007). The high surface area to volume ratio of nanofibrils, compared to wood fibres, results in an enhanced ability to form a tight network with strong interfibrillar bonds and significantly improved mechanical properties (Henriksson *et al.*, 2008). On the other hand, the tendency of nanofibrils to aggregate makes it more difficult to process and produce nanofibril-based materials in larger quantities.
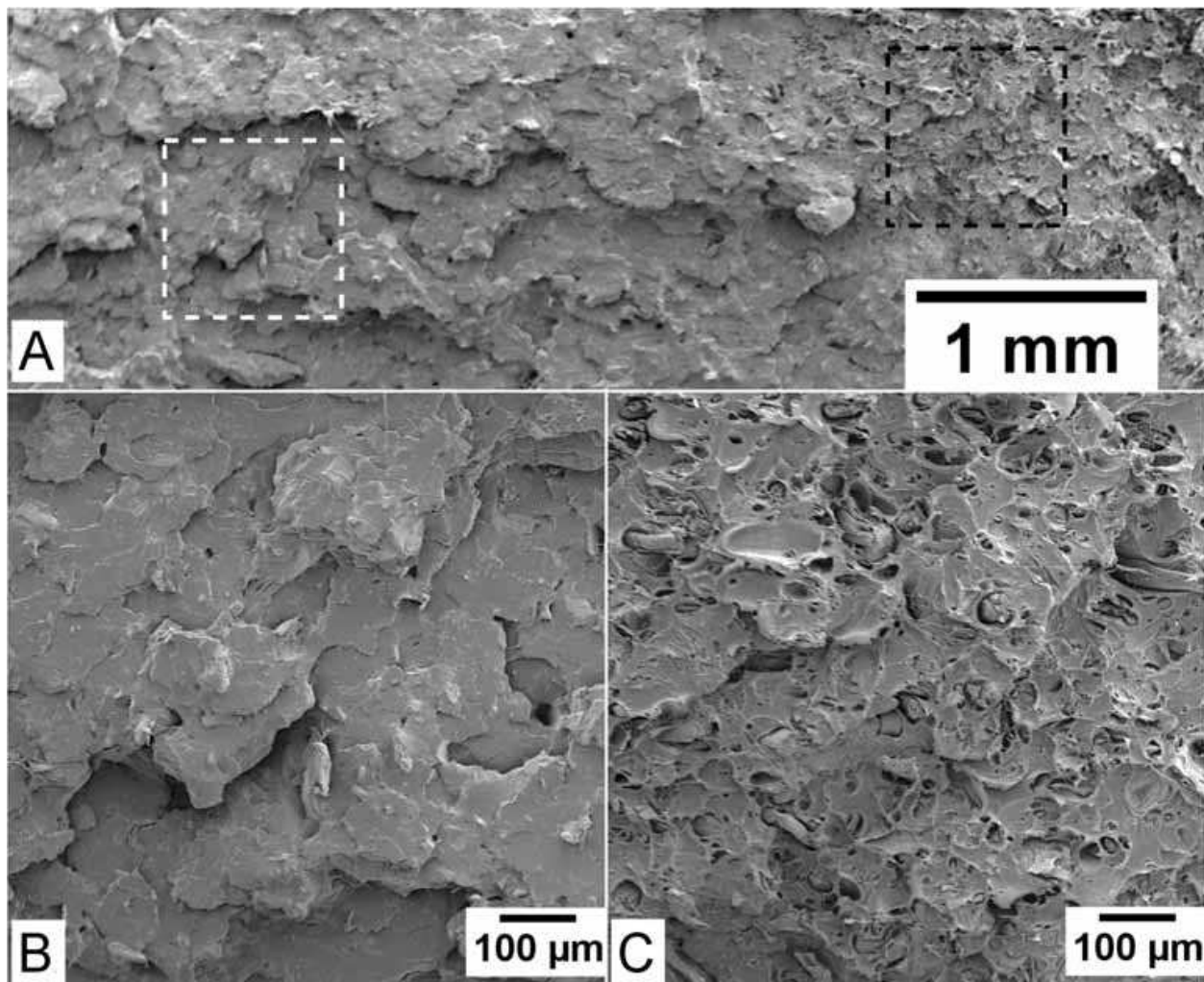
Fig. 8. SEM-SEI imaging of a fracture area. (A) Fracture area after a tensile testing of a kraft fibre-reinforced PLA composite. Facture areas corresponding to the areas marked with white (B) and black (C) dashed rectangles in (A). Note the differences with respect to the fibre spatial distributions in the two fracture areas.

Concerning the reinforcement itself, the stiffness is considerably higher for nanofibrils than wood fibres, since the reinforcing cellulose is aligned in the direction of the nanofibrils. For wood fibres, the cellulose microfibrils have chiral orientation in the cell wall with an inclination angle given by the microfibril angle (MFA). The lumen and softer wood polymers like lignin and hemicellulose also contribute to the lower stiffness of the wood fibres. Cheng *et al.* (2009) have estimated the stiffness of single fibrils to 84 ± 23 GPa by three-point bending in an atomic force microscope, compared with tensile stiffness values 10-25 GPa of various wood pulp fibres (Leopold, 1966). Based on the same arguments, the strength of nanofibrils should be considerably higher than that of wood fibres, although the former is extremely difficult to test, due to the miniscule dimensions of cellulose nanofibrils. Furthermore, nanofibrils are relatively uniform and have fewer defects compared to the corresponding wood fibres. This property contributes to an increased strength, provided that the fibrillation process does not induce damage and degradation of the crystalline nanostructure.

Cellulose nanofibrils have thus a great potential as reinforcement, although the processing challenges should be overcome in order to upscale the production. The small dimensions of nanofibrils (diameter 3.5-100 nm) make them almost impossible to be distinguished in presently utilized X-μCT techniques. Hence, high-resolution electron microscopy must generally be used to estimate the dimensions of a given nanofibril material. However, with further development of tomographic and microscopic characterization techniques, the nanostructure-property relations could be addressed from a mechanistic viewpoint, similarly to the microstructure-property relations of wood-fibre composites.

The long-term goal is to conceive useful methods to quantify microstructural parameters of wood-fibre composites that affect relevant engineering properties. Additionally, models that link these microstructural parameters to the mechanical properties should be developed. Some methods can be borrowed from work on short-fibre composites based on glass or carbon fibres, although the special characteristics of wood fibres should be taken into account. Such characteristics include; (i) wood fibres are generally not straight and uniform, (ii) wood fibre properties depend on the moisture content, (iii) wood fibres may form strong inter-fibre hydrogen bonds and thus create networks, and (iv) the mechanical properties of wood fibres depend on their corresponding microfibril angle.

6. Conclusions

Given the importance of wood pulp fibres in several renewable applications it has been considered most important to develop and demonstrate adequate methods for characterising their complex morphology and assess how fibre structures are affected by specific processes. In this respect we have focused on practical and complementary imaging (X-μCT and FESEM) and the corresponding image analysis techniques necessary to quantify a given structure.

We have demonstrated that X-μCT is most appropriate for exploring non-destructively the surface and bulk structures of fibre-reinforced composites. As a case study, we described a novel method for measuring the fibre length distribution in a kraft fibre-PLA composite. The results revealed a significant reduction of the fibre length from >1500 μm to <200 μm, which could impose a limitation in the proper application of wood fibres as reinforcement in biodegradable composites. In addition, we have demonstrated how strength properties of a given composite may be reduced due to defects caused by relatively large fibre agglomerates. This new insight has been possible due to the non-destructive capabilities of X-μCT, which facilitates the visualization of a composite specimen before and after mechanical testing. The effect of other key microstructural parameters, such as fibre length, orientation and relative content on mechanical properties have also been discussed.

This chapter has also emphasized the applicability of various scanning electron microscopy (SEM) techniques. SEM analyses can be performed in backscatter electron imaging and secondary electron imaging modes for quantification of fibre cross-sectional dimensions and assessment of fracture areas, respectively. In addition, the resolution power of modern field-emission SEM (FESEM) expands and complements structural studies of wood fibre structures and their nanofibrillated materials. A potential method for quantification of cellulose nanofibril length has been described. Such methods are most important for quality control of nanofibrillated materials and for expanding our understanding of structure-property relationships of fibre/ nanofibril-reinforced composites.

7. Acknowledgement

8. References

Abe, K.; Iwamoto, S. & Yano, H. (2007). Obtaining cellulose nanofibers with a uniform width of 15 nm from wood. *Biomacromolecules,* Vol. 8, pp. 3276-3278.

Ahola, S.; Salmi, J.; Johansson, L.-S.; Laine, J. & Österberg, M. (2008). Model films from native cellulose nanofibrils. Preparation, swelling, and surface interactions. *Biomacromolecules,* Vol. 9, pp. 1273-1282.

Alemdar, A.; Zhang, H.; Sain, M.; Cescutti, G. & Müssig, J. (2008). Determination of Fiber Size Distributions of Injection Moulded Polypropylene/ Natural Fibers Using X-ray Microtomography. *Advanced Engineering Materials*, Vol. 10, Nos. 1-2, pp. 126-130.

Almgren, K.M.; Gamstedt, E.K. & Varna, J. (2010). Contribution of Wood Fiber Hygroexpansion to Moisture Induced Thickness Swelling of Composite Plates. *Polymer Composites*, Vol. 31, No. 5, pp. 762-771.

Axelsson M. (2008). Estimating 3D fibre orientation in volume images. In Proc. Of 19th Int. Conf. Pattern Recognition, Tampa, Florida, USA.

Axelsson, M. (2009). Image Analysis for Volumetric Characterisation of Microstructure. PhD thesis, Swedish University of Agricultural Sciences, Uppsala, Sweden.

Cheng, Q.; Wang, S.; Harper, D. (2009). Effects of Process and Source on Elastic Modulus of Single Cellulose Fibrils Evaluated by AFM. *Composites Part A*, Vol. 40, No. 5, pp. 583-588.

Chinga-Carrasco, G.; Lenes, M.; Johnsen, P.O. & Hult, E.-L. (2009). Computer- assisted scanning electron microscopy of wood pulp fibres: dimensions and spatial distributions in a polypropylene composite. Micron, Vol. 40, No. 7, pp. 761-768.

Chinga-Carrasco, G.; Johnsen, P.O. & Øyaas, K. (2010). Structural quantification of wood fibres surfaces – morphological effects of pulping and enzymatic treatment. *Micron,* Vol. 41, No. 6, pp. 648-659.

Chinga-Carrasco, G.; Yu, Y. & Diserud, O. (2011). Quantitative electron microscopy of cellulose nanofibril structures from Eucalyptus and Pinus radiata kraft pulp fibres. *Microscopy and microanalysis*. In Press, Vol. 17, No. 4.

Cox, H.L. (1952). The Elasticity and Strength of Paper and Other Fibrous Materials, *British Journal of Applied Physics*, Vol. 3, No. 2, pp. 72-79.

Czepkowshi, T.; Sówko, W. (1996). Some limitations of surface profile reconstruction in scanning electron microscopy. *Scanning,* Vol. 18, No. 6, pp. 433-446.

de Silveira, G.; Forsberg, P. & Conners, T.E. (1995). Scanning electron microscopy: a tool for the analysis of wood pulp fibres and paper. *In Surface analysis of paper*. Ed. Terrance E. Conners, Sujit Banerjee, Boca Raton, CRC Press.

Duchesne, I. & Daniel, G. (2000). Changes in surface ultrastructure of Norway spruce fibres during kraft pulping - visualization by field emission-SEM. *Nordic Pulp Paper Resources Journal,* Vol. 15, No. 1, pp. 54-61.

Fowler, P.A.; Hughes, J.M. & Elias, R.M. (2006). Biocomposites: Technology, Environmental Credentials and Market Forces, *Journal of the Science of Food and Agriculture*, Vol. 86, No. 12, pp. 1781-1789.

Structural Characterisation of Kraft Pulp Fibres and Their
Nanofibrillated Materials for Biodegradable Composite Applications

259

Fukuda, H. & Chou, T.-W. (1981). A Probabilistic Theory for the Strength of Short Fibre Composites. *Journal of Materials Science*, Vol. 16, No. 4, pp. 1088-1096,

Gonzalez, R. C., Woods, R. E. (2002). *Digital Image Processing* (Second edition)*,* Prentice Hall, ISBN 0-130-94650-8, USA.

Hein, L.R.O. (2001) Quantitative fractography by digital image processing: NIH Image macro tools for stereo pair analysis and 3-D reconstruction. *Journal Microscopy,* Vol. 204, pp. 17– 28.

Henriksson, M.; Henriksson, G.; Berglund, L.A. & Lindström, T. (2007). An Environmentally Friendly Method for Enzyme-Assisted Preparation of Microfibrillated Cellulose (MFC) Nanofibers. *European Polymer Journal*, Vol. 43, No. 8, pp. 3434-3441.

Henriksson, M.; Berglund, L.A.; Isaksson, P.; Lindström, T. & Nishino, T. (2008). Cellulose Nanopaper Structures of High Toughness. *Biomacromolecules*, Vol. 9, No. 6, pp. 1579-1585.

Herrick, F.W.; Casebier, R.L.; Hamilton, J.K. & Sandberg, K.R. (1983). Microfibrillated Cellulose: Morphology and accessibility. *Journal Applied Polymer Science, Applied Polymer Symposium,* Vol. 37, pp. 797-813.

Heyn, A.N. (1969). The elementary fibril and supermolecular structure of cellulose in soft wood fiber. *Journal Ultrastructure research,* Vol. 26, pp. 52-68.

Holmstad, R.; Gregersen, Ø.W.; Aaltosalmi, U.; Kataja, M.; Koponen, A.; Goel, A. & Ramaswamy, S. (2005). Comparison of 3D structural characteristics of high and low resolution X-ray microtomographic images of paper. *Nordic Pulp and Paper Research Journal,* Vol. 20, No. 3, pp. 283-288.

Jähne, B. (2002). *In Digital Image Processing*. Springer, Berlin.

Klemm, D.; Kramer, F.; Moritz, S.; Lindström, T.; Ankerfors, M.; Gray, D. & Dorris, A. (2010). Nanocellulose: A new Family of Nature – Based Materials*. Green nanomaterials*, DOI: 10.1002/ anie.200.

Leopold, B. (1966). Effect of Pulp Processing on Individual Fibre Strength, *TAPPI*, Vol. 49, No. 7, pp. 315-318.

Luengo Hendriks, C.L. (2004). *Structure Characterization Using Mathematical Morphology*. PhD Thesis, Delft University of Technology, The Netherlands.

Luengo Hendriks, C.L. (2010). Constrained and Dimensionality-Independent Path Openings. *IEEE Transactions on Image Processing,* Vol. 19, No. 6, pp. 1587-1595.

Matheron, G. (1975). *Random Sets and Integral Geometry*. Wiley, New York.

McCoy, R.A. (1994). SEM Fractography and Failure Analysis of Nonmetallic Material. *Journal of failure analysis and prevention,* Vol. 4, No. 6, pp. 58-64.

McHenry, E. & Stachurski, Z.H. (2003). Composite Materials Based on Wood and Nylon Fibre. *Composites Part A.*, Vol. 34, No. 2, pp. 171-181.

Meier, H. (1962). Chemical and morphological aspects of the fine structure of wood. *Pure applied chemistry,* Vol. 5, pp. 37-52.

Miettinen, A.; Luengo Hendriks, C.; Chinga-Carrasco, G.; Gamstedt, E.K. & Kataja, M. (2011). A non-destructive X-ray microtomography approach for measuring fibre length in short-fibre composites. Submitted for publication.

Mörseburg, K. & Chinga-Carrasco G. (2009). Assessing the combined benefits of clay and nanofibrillated cellulose in layered TMP-based sheets. Cellulose, Vol. 16, No. 5, pp. 795-806.

Nordin, L.-O. (2004). *Wood Fiber Composites: From Processing and Structure to Mechanical Performance*, PhD thesis, Luleå University of Technology, ISSN 1402-1544

Nygård, P.; Tanem, B.S.; Karlsen, T.; Brachet, P. & Leinsvang, B. (2008). Extrusion-based wood fibre-PP composites: Wood powder and pelletized wood fibres – a comparative study. *Composites Science and Technology*, Vol. 68, No. 15-16, pp. 3418-3424.

Piggott, M.R. (1970). Theoretical Estimation of Fracture Toughness of Fibrous Composites. *Journal of Materials Science*, Vol. 5, No. 8, pp. 669-675.

Pääkkö, M.; Ankefors, M.; Kosonen, H.; Nykänen, A.; Ahola, S.; Österberg, M.; Ruokolainen, J.; Laine, J.; Larsson, P.T.; Ikkala, O. & Lindström, T. (2007). Enzymatic hydrolysis combined with mechanical shearing and high-pressure homogenization for nanoscale cellulose fibrils and strong gels. *Biomacromolecules,* Vol. 8, 1934-1941.

Reme, P.A.; Johnsen, P.O. & Helle, T. (2002). Assessment of fibre transverse dimensions using SEM and image analysis. *Journal of Pulp and Paper Science,* Vol. 28, No. 4, pp. 122-128.

Saito, T.; Nishiyama, Y.; Putaux, J.L.; Vignon, M. & Isogai, A. (2006). Homogeneous Suspensions of Individualized Microfibrils from TEMPO-Catalyzed Oxidation of Native Cellulose. *Biomacromolecules,* Vol. 7, No. 6, pp. 1687-1691.

Samuelsen, E.J; Helle, T.; Houen, P.-J.; Gregersen, Ø.W. & Raven, C. (2001). Three dimensional imaging of paper by use of synchrotron X-ray microtomography. *Journal of Pulp and Paper Science,* Vol. 27, No. 2, pp. 50-53.

Smith, S.M. & Brady, J.M. (1997). SUSAN – a new approach to low level image processing. *International Journal of Computer Vision,* Vol. 23, No. 1, pp. 45-78.

Soille, P. (2003). *Morphological Image Analysis*, 2nd ed. Springer, Berlin.

Syverud, K.; Chinga-Carrasco, G.; Toledo, J & Toledo, P. (2010). A comparative study of *Eucalyptus* and *Pinus radiata* pulp fibres as raw materials for production of cellulose nanofibrils. *Carbohydrate Polymers*, Vol. 84, No. 3, pp. 1033-1038.

Tomasi, C. & Manduchi, R. (1998). Bilateral filtering for gray and color images. *Proceedings of the sixth IEEE International Conference on Computer Vision*, ISBN 81-7319-221-9, India, January 1998.

Turbak, A.F.; Snyder, F.W. & Sandberg, K.R. (1983). Microfibrillated cellulose, a new cellulose product: properties, uses, and commercial potential. *Journal of Applied Polymer Science, Applied Polymer Symposium*, Vol. 37, pp. 815–827.

Verbeek, P.W.; Verwer, B.JH. (1990). Shading from shape, the eikonal equation solved by grey-weighted distance transform. *Pattern Recognition Letters* Vol. 11, pp. 681-690.

Vossepoel, A.M.; Smeulders, A.W.M. (1982). Vector code probability and metrication error in the representation of straight lines of finite length. *Computer Graphics and Image Processing,* Vol. 20, No. 4, pp. 347-364.

Wågberg, L.; Decher, G.; Norgren, M.; Lindström, T.; Ankerfors, M. & Axnas, K. (2008). The build-up of polyelectrolyte multilayers of microfibrillated cellulose (MFC) and cationic polyelectrolytes. *Langmuir,* Vol. 24, pp. 784-795.

Zhang, R.; Tsai, P.-S.; Cryer, J.E.; Shah, M. (1999). Shape from Shading: A Survey. *IEEE Transactions on Image Processing,* Vol. 21, No. 8, pp. 690-706.
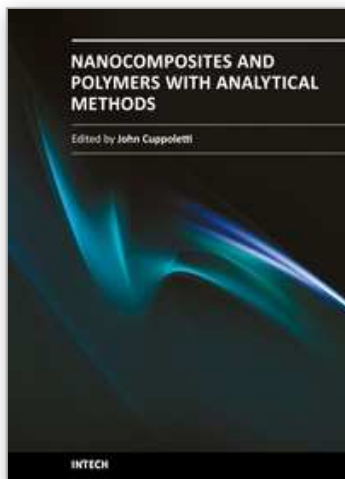
This book contains 16 chapters. In the first part, there are 8 chapters describing new materials and analytic methods. These materials include chapters on gold nanoparticles and Sol-Gel metal oxides, nanocomposites with carbon nanotubes, methods of evaluation by depth sensing, and other methods. The second part contains 3 chapters featuring new materials with unique properties including optical non-linearities, new materials based on pulp fibers, and the properties of nano-filled polymers. The last part contains 5 chapters with applications of new materials for medical devices, anodes for lithium batteries, electroceramics, phase change materials and matrix active nanoparticles.

How to reference

In order to correctly reference this scholarly work, feel free to copy and paste the following:

Gary Chinga-Carrasco, Arttu Miettinen, Cris L. Luengo Hendriks, E. Kristofer Gamstedt and Markku Kataja (2011). Structural Characterisation of Kraft Pulp Fibres and Their Nanofibrillated Materials for Biodegradable Composite Applications, Nanocomposites and Polymers with Analytical Methods, Dr. John Cuppoletti (Ed.), ISBN: 978-953-307-352-1, InTech, Available from: http://www.intechopen.com/books/nanocomposites-and-polymers-with-analytical-methods/structural-characterisation-of-kraft-pulp-fibres-and-their-nanofibrillated-materials-for-biodegradab